

Reduced kinetic description of weakly-driven plasma waves^{a)}

R. R. Lindberg,^{b)} A. E. Charman, and J. S. Wurtele

Department of Physics, University of California, Berkeley, Berkeley, California 94720, USA

and Center for Beam Physics, Lawrence Berkeley National Laboratory, Berkeley, California 94720, USA

(Received 16 November 2007; accepted 20 March 2008; published online 28 May 2008)

A model of kinetic effects in Langmuir wave dynamics is presented using a nonlinear distribution function that includes particle separatrix crossing and self-consistent electrostatic evolution. This model is based on the adiabatic motion of electrons in the wave to describe Bernstein–Greene–Kruskal-like Langmuir waves over a wide range of temperatures ($0.1 \leq k\lambda_D \leq 0.4$). The asymptotic distribution function yields a nonlinear frequency shift of the Langmuir wave that agrees well with Vlasov simulations, and can furthermore be used to determine the electrostatic energy required to develop the phase-mixed, asymptotic state. From this incoherent energy, energy conservation is employed to determine a simplified model of nonlinear Landau damping. The resulting nonlinear, dynamic frequency shift and damping are then used in an extended three-wave-type model of driven Langmuir waves and compared to Vlasov simulations in the context of backward Raman scattering. © 2008 American Institute of Physics. [DOI: 10.1063/1.2907777]

I. INTRODUCTION

Kinetic effects play a central role in plasma physics. Linear plasma kinetic theory has had a long history, including such central effects as Landau damping. For sufficiently large amplitude excitations, however, other effects, including the nonlinear reduction of Landau damping¹ and the existence of long-lived nonlinear modes (Bernstein–Greene–Kruskal modes²), can become relevant. Recently, it has been demonstrated both experimentally^{3,4} and numerically^{5–7} that kinetic effects involving nonlinear modifications to the distribution function can be relevant to Raman backscatter (RBS) in a plasma. A recently identified promising application of resonant Raman Backscattering in plasma is laser pulse compression,⁸ the advantage of plasma being its ability to tolerate much higher laser intensities than solid-state elements. Understanding kinetic effects is important to determine the overall amplifier;⁹ computational codes have indicated that plasma kinetics can significantly reduce pulse amplification,¹⁰ and it appears to play an important role in recent experiments.¹¹ To fully address these issues theoretically, one must turn to either particle-in-cell or Vlasov simulation tools. Even with increasing computational power, however, full-scale kinetic simulations in multiple dimensions are often prohibitively time-consuming. Furthermore, it is useful to have a simplified picture that encapsulates the underlying physics. For these reasons, in this paper we explore one such reduced description of kinetic effects. Although our enhanced coupled-wave model shares the basic phenomenology presented in, e.g., Refs. 12–14, it explicitly uses the properties of the phase-mixed, nonlinear state that results after many particle oscillations.

Our model assumes that the plasma electrons move adiabatically in a slowly evolving potential dominated by the

self-consistent electrostatic field. This implies that the time rate of change of the plasma wave is slow with respect to the plasma frequency $\omega_p \equiv \sqrt{4\pi e^2 n_0 / m_e}$ (with n_0 the equilibrium plasma density, and e , m_e the magnitude of the electron charge and mass, respectively), while the amplitude is sufficiently large so that the ponderomotive force arising from the counterpropagating lasers can be neglected for individual particle motion. The latter constraint is relatively unimportant for the plasma temperatures considered here, but as shown by Ref. 15, the ponderomotive force significantly modifies the distribution function such that natural plasma modes can exist for temperatures with $k\lambda_D > 0.53$, where the Debye length $\lambda_D \equiv v_{th} / \omega_p$ and v_{th} is the thermal speed.

We present the reduced equations of RBS in Sec. II, for which the counterpropagating lasers are described by two first-order envelope equations, coupled by the lowest-order harmonic of the plasma wave potential. The Langmuir wave in turn is governed by an envelope equation whose frequency and damping we calculate in two physically relevant limits: the first corresponds to the initial, linear stage characterized by the Landau damped solution; the second is given by a time-asymptotic, phase-mixed state whose damping vanishes while the particles trapped in the slowly growing Langmuir wave give rise to a nonlinear frequency shift. The physics of this reduced damping and nonlinear frequency were provided by O’Neil and Morales^{1,16} and by Dewar,¹⁷ and the resulting distribution function was described in Ref. 18. To complete our model, in Sec. III we approximate the degree of phase-mixing using the ratio of the dynamically damped energy to that required to develop the asymptotic state, thereby providing a heuristic but physically meaningful method of transitioning between the two limits. In Sec. IV, we compare the dynamics of our extended envelope model to those of full Vlasov simulations in both the driven and fully coupled case associated with RBS.

^{a)}Paper CII 1, Bull. Am. Phys. Soc. 52, 58 (2007).

^{b)}Invited speaker.

II. COUPLED MODE EQUATIONS OF RBS

We imagine two counterpropagating lasers whose envelopes have slow spatiotemporal variation with respect to the phase of the wave, so that the vector potential is

$$\begin{aligned} \mathbf{A}(z, t) \equiv & \frac{m_e c^2}{e} \mathbf{a}_\perp = \frac{m_e c^2}{e \sqrt{2}} a_0(z, t) e^{-i(\omega_0 t + k_0 z)} \hat{\mathbf{x}} \\ & + \frac{m_e c^2}{e \sqrt{2}} a_1(z, t) e^{-i(\omega_1 t - k_1 z)} \hat{\mathbf{x}} + \text{c.c.}, \end{aligned} \quad (1)$$

where a_0 and a_1 are the dimensionless rms laser amplitudes and c is the speed of light. We assume that the ions are stationary over the time scales of interest, while the transverse variation is sufficiently slow that the system is approximately one-dimensional along z . Thus, conservation of canonical momentum implies that the transverse current $-en_e \mathbf{v}_\perp = -en_e c \mathbf{a}_\perp$. Finally, we assume that the laser envelopes vary slowly with respect to their phase, and average the Ampère–Maxwell law over the fine spatial scale $\sim 1/k_{0,1}$ and the fast time scale $\sim 1/\omega_{0,1}$; details of this averaging can be found in, for example, Ref. 19. We normalize time by the plasma frequency ω_p and distance by the beat wave vector $k_2 \equiv k_0 + k_1$, assuming that k_2 is essentially constant. We introduce the dimensionless space-time coordinates (ζ, τ) , the scaled frequency difference ω_L , and group velocities u_0, u_1 via

$$\zeta \equiv k_2 z, \quad \tau \equiv \omega_p t,$$

$$\omega_L \equiv \frac{\omega_0 - \omega_1}{\omega_p}, \quad u_0 \equiv \frac{k_2 c^2 k_0}{\omega_p \omega_0}, \quad u_1 \equiv \frac{k_2 c^2 k_1}{\omega_p \omega_1},$$

finding it convenient to choose the frequency difference ω_L to satisfy the Vlasov dispersion relation (10), with any slow difference in the wave frequencies being accounted for by the complex envelopes. With these definitions, the averaged Ampère–Maxwell law yields the following set of coupled laser amplitude equations:

$$\left[\frac{\partial}{\partial \tau} - u_0 \frac{\partial}{\partial \zeta} \right] a_0 = - \frac{i \omega_p}{2 \omega_0} a_1 \langle e^{i(\omega_L \tau + \zeta)} \rangle, \quad (2a)$$

$$\left[\frac{\partial}{\partial \tau} + u_1 \frac{\partial}{\partial \zeta} \right] a_1 = - \frac{i \omega_p}{2 \omega_1} a_0 \langle e^{-i(\omega_L \tau + \zeta)} \rangle, \quad (2b)$$

where we have defined the ponderomotive wavelength, phase space average of the quantity \mathcal{X} to be

$$\langle \mathcal{X} \rangle(\zeta, \tau) \equiv \frac{1}{2\pi} \int_{\zeta-\pi}^{\zeta+\pi} d\zeta' \int_{-\infty}^{\infty} du f(u, \zeta', \tau) \mathcal{X}(u, \zeta', \tau)$$

in terms of the dimensionless phase space coordinates $u \equiv k_2 v / \omega_p$ and $\zeta \equiv k_2 z$. To complete the three-wave model of RBS requires a mode equation for the averaged ponderomotive phase $\langle e^{i(\omega_L \tau + \zeta)} \rangle$. Such an equation can be derived by expanding the linear-response function assuming that the plasma varies slowly in space and time (see, e.g., Ref. 20, Chap. 7), or by directly considering phase-averaged moments of the Vlasov equation (as is done in Ref. 22). The upshot of these analyses is that the lowest-order plasma re-

sponse is governed by an advection equation with a slowly varying frequency and damping. We find that the dominant plasma mode

$$g(\zeta, \tau) \equiv -2i \langle e^{i(\omega_L \tau + \zeta)} \rangle \quad (3)$$

obeys the following Langmuir wave envelope equation:

$$\left[\frac{\partial}{\partial \tau} - u_2 \frac{\partial}{\partial \zeta} + i(\omega - \omega_L) + \nu \right] g = - \frac{c^2 k_2^2}{2 \omega_L \omega_p^2} a_0 a_1^*, \quad (4)$$

where we have introduced the dimensionless, linear plasma group velocity $u_2 \equiv k_2 (\partial \omega / \partial k_2)$ and neglected frequency shifts in the ponderomotive coupling. The (real, dimensionless) Langmuir wave frequency ω and damping ν depend on the distribution function and are, in general, nonlinear (and possibly nonlocal) functions of the wave amplitude $|g|$. Furthermore, we consider these to be properties of the plasma independent of the drive, and as such they are the “natural” or “undriven” values. This is to be contrasted with, e.g., the works of Rose and Russell²¹ and Bénisti and Gremillet,¹⁵ in which “the frequency” is extracted from the simplified SRS plasma dispersion relation $1 + \Re[\chi(\omega)] = 0$, where χ is the plasma susceptibility. The frequency associated with this growing mode can be obtained from Eqs. (2b) and (4) by assuming that a_1 and g are exponential functions $\sim e^{(\gamma - i\Omega)\tau}$ and taking a_0 prescribed; solving the resulting algebraic equation yields exponential growth characterized by γ and a shift in frequency from ω_L by Ω . If the gain is small, $\Omega \approx 0$ and the linear frequency of the growing mode is nearly ω_L as was first discussed in Ref. 21. In the following two subsections, we calculate ω and ν in two physically important limits: That corresponding to the initial value, linear problem; and that of the time-asymptotic distribution, for which the electrons have phase-mixed in the slowly growing wave.

A. Langmuir wave in the initial-value, linear limit

We assume that the plasma is initially Maxwellian with a dimensionless thermal spread given by $\sigma \equiv k_2 \lambda_D$. For linear perturbations, it is well known that the complex frequency $\omega_c \equiv \omega_r - i\nu_\ell$ of the Langmuir wave is given by the solution to the Landau dispersion relation,

$$\frac{1}{\sigma \sqrt{2\pi}} \frac{\partial}{\partial \omega_c} \left[\mathcal{P} \int dx \frac{e^{-x^2/2}}{x - \omega_c / \sigma} + i\pi e^{-\omega_c^2/2\sigma^2} \right] = 1, \quad (5)$$

where \mathcal{P} denotes the Cauchy principal value. Using the complex frequency ω_c in the Langmuir envelope equation (4) yields the familiar driven plasma wave that also experiences linear Landau damping. Again, the unstable RBS wave appears as the linear solution of Eqs. (2b) and (4), which can be shown to oscillate nearly at ω_L as it grows.

As was shown by O’Neil,¹ however, the solution associated with (5) holds only if the wave is damped to zero before the trapped electrons have time to oscillate in the Langmuir potential. If the wave is of sufficiently large amplitude or is

driven/unstable, trapped electrons typically complete one oscillation in the wave on a time scale given by the bounce frequency $\omega_B \equiv \sqrt{|g|}$. Since electrons with different energies have different frequencies in the nearly sinusoidal potential, the electrons then phase-mix in the wave, which in turn flattens the distribution function near the phase velocity, thereby decreasing Landau damping. Furthermore, the nonlinear change to f also gives rise to a shift in the frequency due to the trapped and nearly trapped electrons. We present a brief discussion of this limit in the following subsection.

B. The time-asymptotic, phase-mixed limit of the adiabatic Langmuir wave

We first briefly review some results of Ref. 18, which discusses the phase-mixed distribution function that arises asymptotically as the electrons oscillate in the slowly evolving Langmuir wave. Pioneering work in this regime was done by Dewar,¹⁷ while the more complete analysis of Bénisti and Gremillet¹⁵ has much in common with that presented here. Our discussion is most transparent in terms of the electron action-angle coordinates (J, Ψ) . We assume that the Langmuir wave changes slowly on the bounce time scale, so that the particles experience a nearly constant Hamiltonian during one oscillation in the wave. In this case, the particle action J is adiabatically conserved, modulo a geometric factor when crossing the separatrix (see, e.g., Refs. 23 and 24).

We consider the electron phase $\theta \equiv \omega_L \tau + \zeta + \xi(\tau)$, where $\xi(\tau)$ is a slowly varying phase shift that will give rise to the nonlinear frequency shift via $d\xi/d\tau \equiv \delta\omega$. For any electron, we then divide the electrostatic field into a slowly varying, zero-mean (over the scale $1/k_2$) component and a slowly varying, nearly dc field as follows:

$$\frac{ek_2}{m\omega_p^2} E_z = - \sum n \phi_n(\tau) \sin(n\theta) + \mathcal{E}_0(\tau). \quad (6)$$

Defining the canonical momentum

$$p \equiv \dot{\theta} - \dot{\xi} - a_z(\tau) \equiv u + \omega_L + \int_{-\infty}^{\tau} d\tau' \mathcal{E}_0(\tau') \quad (7)$$

and assuming that the electrostatic force dominates the ponderomotive force, the equations of motion are obtained from the following Hamiltonian:

$$\mathcal{H}(p, \theta; \tau) = \frac{1}{2} [p + \delta\omega(\tau) + a_z(\tau)]^2 - \sum_n \phi_n(\tau) \cos(n\theta).$$

As can be seen from \mathcal{H} , the canonical coordinates were chosen such that the action $J \equiv \oint d\theta p(\mathcal{H}, \theta)/2\pi$ is an adiabatic invariant of motion, so that the distribution function remains essentially invariant in action under slow evolution. Furthermore, as time progresses the particles phase-mix in the pendulum-like potential, so that the asymptotic distribution function becomes essentially uniform in the canonical angle and invariant in the canonical action. It is this property that permits us to uniquely characterize f as a function solely of

the amplitude $|g| = \phi_1$; to do so, we require that the invariant-in-action distribution give rise to the corresponding electrostatic potential via Maxwell's equations. From the Fourier transformed Poisson equation, we have

$$\phi_n = - \frac{2}{n^2} \langle \cos(n\theta) \rangle, \quad (8)$$

while the wavelength averaged \hat{z} component of the one-dimensional (1D) Ampère–Maxwell law can be written as

$$\delta\omega(\tau) = \left\langle \frac{d\theta}{d\tau} \right\rangle - \omega_L. \quad (9)$$

Taking a finite number of harmonics N , we consider Eqs. (8) and (9) to be $N+1$ equations for the $N-1$ harmonics ϕ_n with $n \geq 2$, the sum $\delta\omega + a_z$, and the frequency shift $\delta\omega$ to be solved as a function of $\phi_1 \equiv |g|$. Taking the linear limit, we find that the natural frequency of the time-asymptotic distribution, denoted by ω_L , is given by the Vlasov dispersion relation,

$$1 + \frac{1}{\sigma^2} \left[1 + \frac{\omega_L/\sigma}{\sqrt{2\pi}} \mathcal{P} \int dx \frac{e^{-x^2/2}}{x - \omega_L/\sigma} \right] = 0. \quad (10)$$

The oscillation frequency ω_L given by Eq. (10) is different from ω_r of the initial value problem because in the latter case the distribution has not yet had time to become uniform in the canonical angle Ψ , i.e., to phase-mix; in the RBS literature, this distinction is sometimes referred to as the “adiabatic” versus “sudden” approximation.

Additionally, as we explicitly show in Ref. 18, in the small-amplitude limit the nonlinear frequency shift is given by

$$\delta\omega = - \eta \omega_L \sqrt{|g|} \frac{(\omega_L^2 - \sigma^2) e^{-\omega_L^2/2\sigma^2}}{\sigma^2 (\omega_L^2 - 1 - \sigma^2) \sqrt{2\pi\sigma}} + \dots, \quad (11)$$

where η is an $O(1)$ constant; similar results to Eq. (11) were first determined by Morales and O’Neil¹⁶ for the initial value problem, and by Dewar¹⁷ and by Rose and Russell²¹ in the identical case of an adiabatically excited wave; we find that $\eta \approx 1.09$, equal to the result of Dewar. For larger amplitude waves, one must solve the implicit equations (8) and (9) to obtain $\delta\omega$. We include plots of the frequency shift for three different temperatures in Fig. 1. The theoretical (solid) lines were determined by solving Eqs. (8) and (9) with eight harmonics, which we compare with the frequencies obtained via a Hilbert transform from a plasma wave that was driven from zero to some nearly constant amplitude, after allowing the distribution to phase-mix. Larger amplitudes of ϕ_1 than those plotted could not be excited due to the nonlinear detuning of the plasma wave from the fixed-frequency drive.

III. THE DYNAMIC FREQUENCY AND DAMPING

We have indicated that driven Langmuir waves can be modeled by the envelope equation (4), whose difference from cold-fluid theory is given by a time- and amplitude-dependent frequency and damping. We then identified two

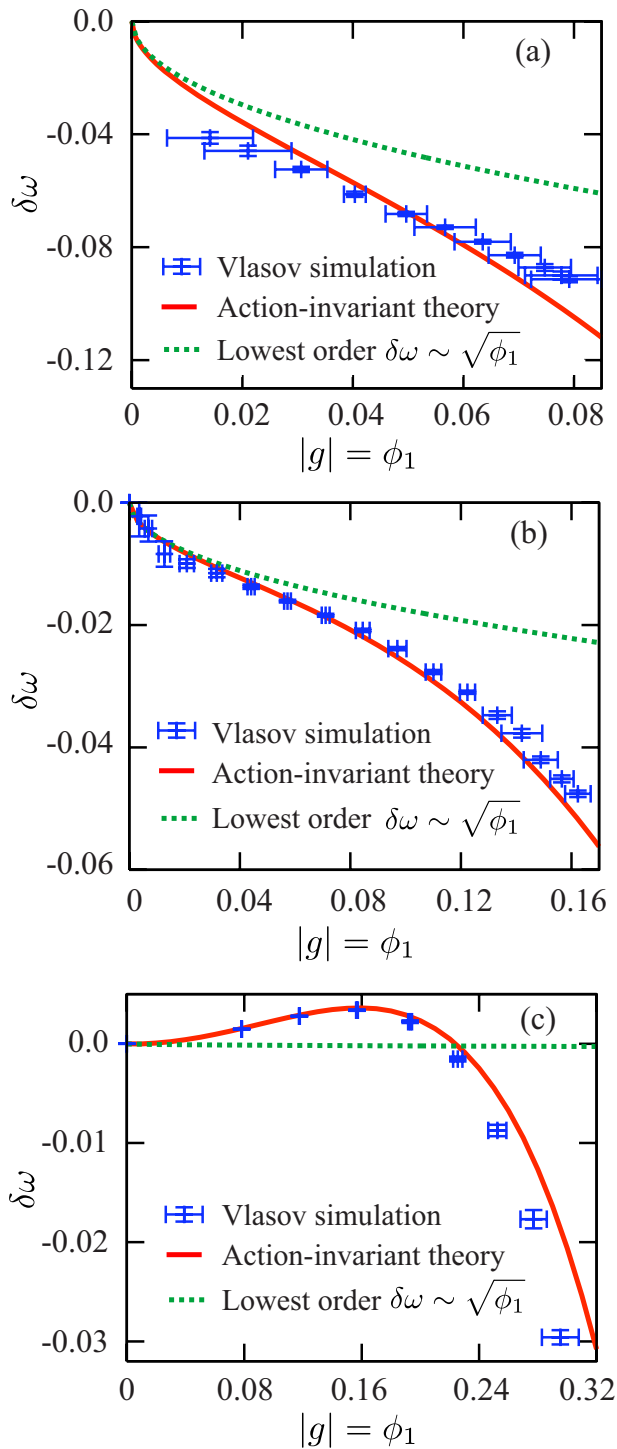


FIG. 1. (Color online) Nonlinear frequency for three different temperatures: $k_2 \lambda_D = 0.4$ (a), 0.3 (b), and 0.2 (c). The prediction of the invariant-in-action theory is the solid line, which agrees well with the nonlinear frequency extracted from Vlasov simulations. For comparison, the lowest-order result Eq. (11) is plotted as a dotted line.

limits for these quantities: The first corresponds to the initial, linear limit, for which we find that the plasma has the natural complex frequency $\omega_r - i\nu_\ell$ of the Landau dispersion relation (5); the second is in the time-asymptotic regime, where particle phase-mixing reduces the damping while giving rise to a nonlinear frequency shift. Schematically, as time progresses we have

$$\begin{aligned} \omega(t=0) &= \omega_r \rightarrow \omega(t=\infty) = \omega_L + \delta\omega, \\ \nu(t=0) &= \nu_\ell \rightarrow \nu(t=\infty) = 0. \end{aligned} \quad (12)$$

The dynamics encapsulated within the arrows of Eq. (12) are complex, involving orbit modification, phase-mixing, and trapping of many particles with disparate initial conditions in an evolving Langmuir wave. If the particles make one bounce oscillation in the wave before its amplitude changes significantly, O'Neil¹ and Morales and O'Neil¹⁶ showed that the damping vanishes while the frequency shift approaches its asymptotic value in a time of order $1/\omega_B$. While our phenomenology is similar, generalizing these results to driven waves of arbitrary amplitudes would complicate our reduced description. Rather, we present a simple model describing the process (12) based on energy conservation: The electrostatic energy that is "lost" due to Landau damping is equal to the kinetic energy gain associated with particle phase-mixing.

The basic physics (energy conservation during particle phase-mixing) of our model is quite similar to O'Neil's, and also has much in common with the work of Dewar,²⁵ who investigated the nonlinear saturation of plasma instabilities via particle trapping and subsequent phase-mixing. We will find that our theory reproduces his analytic result in the small-amplitude limit. For larger-amplitude potentials, however, we require the full asymptotic phase-mixed distribution described in Sec. II B.

A. Energy conservation and phase-mixing

We use two expressions for the energy: The first from the envelope equation (4), the second from the Vlasov equation. Equating these yields the incoherent, phase-mixed energy required to develop the asymptotic distribution of Sec. II B, which we will see is built up over time by Landau-type damping. To begin, we multiply Eq. (4) by $\omega_L^2 g^*/2$ and add its complex conjugate,

$$\begin{aligned} \left[\frac{\partial}{\partial \tau} - u_2 \frac{\partial}{\partial \zeta} + 2\nu(|g|, \tau) \right] \frac{1}{2} \omega_L^2 |g|^2 \\ = -\omega_L \frac{c^2 k_2^2}{4\omega_p^2} (a_0^* a_1 g + a_0 a_1^* g^*). \end{aligned} \quad (13)$$

Equation (13) describes how the wave energy (i.e., the product of the wave action density/quanta $\omega_L |g|^2$ and its excitation energy ω_L) evolves in time. The second term on the left-hand side advects the energy in space, while the third term decreases it through a (possibly nonlinear) Landau-type damping; the right-hand side couples the Langmuir energy to the lasers via the product of the effective ponderomotive current $a_0 a_1$ with the electrostatic field g . To eliminate this driving term, we use the expression of energy conservation derived from the Vlasov equation,

$$\frac{\partial}{\partial \tau} \left\{ \left\langle \frac{1}{2} u^2 \right\rangle + \frac{1}{4} |g|^2 + \sum_{n=2}^{\infty} \frac{n^2}{4} |\phi_n|^2 \right\} + \frac{\partial}{\partial \zeta} \left\langle \frac{1}{2} u^3 \right\rangle = -\omega_L \frac{c^2 k_2^2}{4\omega_p^2} (a_0^* a_1 g + a_0 a_1^* g^*). \quad (14)$$

The quantity in curly brackets gives the time rate of change of the kinetic plus potential energies, the first term on the second line is the flux, and the right-hand side is the lowest-order coupling of the ponderomotive current and the longitudinal field, where we neglect terms $\sim \partial_\tau g$ assuming that the wave grows adiabatically so that $|\partial_\tau \ln g| \ll 1$.

The ponderomotive coupling is eliminated by equating the left-hand sides of Eqs. (14) and (13). Considerations of local energy conservation suggest that the energy flux terms should also be equal; we explicitly show this to be true in the small-amplitude, low-temperature limit, for which the plasma group velocity $u_2 \approx \omega_L^2 - 1$. Linearizing the distribution function via $f = f_0 + f_1$, with f_0 Maxwellian and $f_1 \ll f_0$, the perturbed distribution is

$$f_1 = -\frac{1}{2} \sum_{n \neq 0} [\phi_n e^{-in(\omega_L \tau + \zeta)} + \text{c.c.}] \frac{\frac{\partial}{\partial u} f_0}{u - \omega_L},$$

so that to lowest order, the third velocity moment is

$$\langle u^3 \rangle \approx \frac{g^*}{2} \int du d\zeta \frac{u^3 \frac{\partial}{\partial u} f_0}{u - \omega_L} e^{i(\omega_L \tau + \zeta)} + \text{c.c.} \approx (\omega_L^2 - 1) |g|^2,$$

and the two energy fluxes from Eqs. (14) and (13) cancel. Integrating over all time, and taking $g = \phi_n = 0$, $\langle u^2 \rangle = \sigma^2$ initially at $t=0$, we find that the integrated damped energy is given by the following relation:

$$\begin{aligned} \omega_L^2 \int_0^\infty d\tau' \nu |g|^2 &= \underbrace{\frac{1}{2} [\langle u^2 \rangle - \sigma^2]}_{(a)} + \underbrace{\frac{1}{4} \left[|g|^2 + \sum_{n=2}^{\infty} n^2 \phi_n^2 \right]}_{(b)} \\ &\quad - \underbrace{\frac{1}{2} \omega_L^2 |g|^2}_{(c)} \\ &\equiv U_{\text{incoh}}. \end{aligned} \quad (15)$$

Thus, the total damped energy equals the incoherent energy associated with complete particle phase-mixing in the (nearly) sinusoidal potential. To be explicit, we split the incoherent energy U_{incoh} into three parts: (a) is the change in kinetic energy of the particles; (b) consists of the total electrostatic energy; while (c) represents the wave energy. Thus, the incoherent, phase-mixed energy is given by the difference between the total [kinetic (a) plus potential (b)] and the wave energy (c). The latter wave energy can be understood as the coherent energy in both the particles and fields of the Langmuir wave. In the cold, linear limit, the scaled frequency $\omega_L \rightarrow 1$, and Eq. (15) indicates that the wave energy is equal to twice the electrostatic energy. Furthermore, in this limit the electrostatic and kinetic energies are the same, so

that their sum equals the wave energy $|g|^2/2$, in agreement with standard results (see, e.g., Ref. 26, Sec. 6.6).

The right-hand side of Eq. (15) can be evaluated for a given potential $\phi_1 = |g|$ using the asymptotic, phase-mixed distribution. In the small-amplitude limit, we can approximate the electron motion as that of the physical pendulum, in which case the action and angle are expressible in terms of elliptic functions (details can be found in Ref. 22). Taylor expansion of the resulting semianalytic expressions for the damped energy yields

$$\frac{1}{2} [\langle u^2 \rangle - \sigma^2] = \frac{\pi \omega_L^2}{2 \sigma^2} \frac{e^{-\omega_L^2/2\sigma^2}}{\sigma \sqrt{2\pi}} \frac{128}{9\pi^2} \phi_1^{3/2} \equiv \nu_\ell \frac{128}{9\pi^2} \phi_1^{3/2}. \quad (16)$$

The physical interpretation of Eq. (16) is clear: The increase in the particle kinetic energy is equal to that dissipated by Landau damping over a time of order the bounce period $1/\sqrt{\phi_1}$. The expression (16) is similar to that derived by O'Neil¹ for the initial value problem, while being exactly derivable from Dewar's expression for the momentum of the trapped particles due to the adiabatic saturation of an instability;²⁵ our analysis extends the saturation energy beyond this small-amplitude regime.

B. A model of the dynamic damping and frequency

In the preceding section, we obtained a fully nonlinear expression for the energy required to develop the asymptotic, phase-mixed state of the Langmuir distribution function. We furthermore demonstrated that this additional incoherent energy is equal to the total integrated energy extracted from the wave in Landau-type damping. At any given time in the Langmuir wave evolution, we approximate the "degree of phase-mixing" to be the ratio of the instantaneous damped energy to the total required to develop the asymptotic state,

$$\text{Degree of phase-mixing} \equiv \Gamma = \frac{\omega_L^2 \int_0^\tau d\tau' \nu(|g|, \tau') |g|^2}{U_{\text{incoh}}}. \quad (17)$$

This simple measure is near zero when there has been insufficient time for the particles to phase-mix, while approaching unity after the trapped particles oscillate in the wave. Thus, for $\Gamma \approx 0$ we have an envelope equation whose frequency is near ω_r and whose damping approaches its maximal value. As time passes and the particles phase-mix, $\Gamma \rightarrow 1$ and our prescription (12) implies that the damping vanishes while the frequency decreases to $\omega_L + \delta\omega$. We smoothly interpolate between these two limits using a hyperbolic tangent function as shown in Fig. 2; note that we have numerically found the model to be relatively insensitive to the somewhat arbitrary choice of interpolating function.

As the wave grows, the effective damping coefficient increases as particles are trapped from deeper in the plasma bulk. To determine the maximal damping rate associated with a plasma wave whose asymptotic, phase-mixed energy is U_{incoh} , we proceed by analogy with the small-amplitude limit, in which we interpreted this energy to be proportional to the electrostatic energy $\sim \phi_1^2$ damped over a bounce period $\sim 1/\sqrt{\phi_1}$. Thus, the behavior of the total Landau damped energy is given by $U_{\text{incoh}} \sim \nu_{\text{max}}(\phi_1) |g|^2$, and the maximal

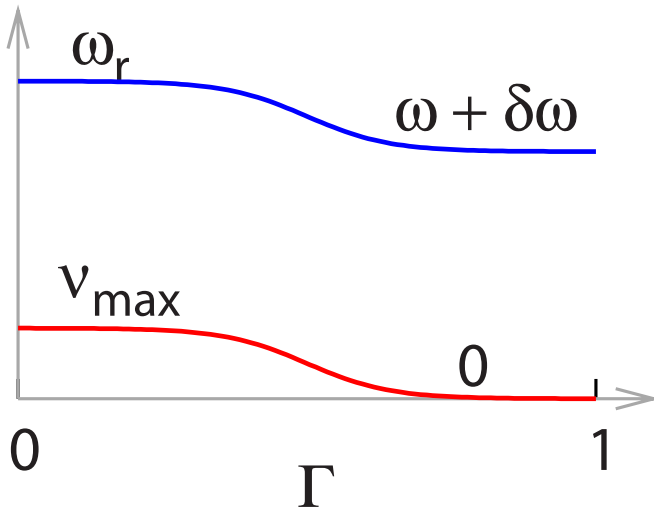


FIG. 2. (Color online) Schematic of the prescription (12) for the damping and frequency as a function of the degree of phase-mixing; we model the degree of phase-mixing by the ratio Γ of the dynamically damped energy to that required to develop the time-asymptotic, phase-mixed state, i.e., Eq. (17).

damping of the plasma wave is proportional to $U_{\text{incoh}}/|g|^{3/2}$. To recover linear Landau damping as $|g| \rightarrow 0$, we use the small-amplitude result (16), finding that

$$\nu_{\text{max}}(\phi_1) = \frac{9\pi^2 U_{\text{incoh}}}{128 \phi_1^{3/2}}. \quad (18)$$

To summarize, our extended three-wave model of kinetic Raman backscatter is given by

$$\left[\frac{\partial}{\partial \tau} - u_0 \frac{\partial}{\partial \zeta} \right] a_0 = \frac{\omega_p}{4\omega_0} a_1 g, \quad (19a)$$

$$\left[\frac{\partial}{\partial \tau} + u_1 \frac{\partial}{\partial \zeta} \right] a_1 = -\frac{\omega_p}{4\omega_1} a_0 g^*, \quad (19b)$$

$$\left[\frac{\partial}{\partial \tau} - u_2 \frac{\partial}{\partial \zeta} + i(\omega - \omega_L) + \nu \right] g = -\frac{c^2 k_2^2}{2\omega_L \omega_p^2} a_0 a_1^*, \quad (19c)$$

where, for $|g| \equiv \phi_1$, we have

$$\nu(\phi_1, \Gamma) = \{1 - \tanh[7(\Gamma - 0.5)]\} \nu_{\text{max}}(\phi_1)/2, \quad (20a)$$

$$\omega(\phi_1, \Gamma) = \{1 - \tanh[7(\Gamma - 0.5)]\} \omega_r/2 + \{1 + \tanh[7(\Gamma - 0.5)]\} [\omega_L + \delta\omega(\phi_1)]/2. \quad (20b)$$

In the model above, the damping ν_{max} is given by Eq. (18), the (real) frequencies ω_r and ω_L are derivable from the Landau and Vlasov dispersion relations, (5) and (10) respectively, the nonlinear frequency shift $\delta\omega$ is obtained via Eq. (9), and the degree of phase-mixing $\Gamma(|g|, \tau)$ is given by Eq. (17), where the numerator is dynamically tracked in the simulation while the denominator is from Eq. (15).

Our set of equations bears some resemblance to that of Vu, DuBois, and Bezzlerides¹³ for RBS and to that of Cohen, Williams, and Vu¹⁴ for Brillouin scattering (with the Langmuir wave replaced by an ion wave). The former considers the competition between trapping (which decreases damping while yielding a nonlinear frequency shift) and collisions (which tends to detrap particles and return the plasma to a Maxwellian). Using physical intuition provided by Zakharov and Karpman²⁷ and O'Neil,¹ Vu *et al.* then obtains thresholds for when to eliminate Landau damping and when to use a frequency shift that matches, within factors of $O(1)$, that of Morales and O'Neil,¹⁶ i.e., Eq. (11). The latter model of Cohen and collaborators employs a similar choice for $\delta\omega$, but uses the integrated bounce time to determine when the damping vanishes and the frequency shift manifests itself. The model we have derived is qualitatively similar to these, but is obtained with a consistent and uniform set of equations and assumptions, and is applicable to larger-amplitude Langmuir waves. For longer time scales, however, our analysis will need to be generalized to include the collisional relaxation of the plasma.

IV. MODEL DYNAMICS AND APPLICATIONS

A. Prescribed ponderomotive forcing

To illuminate the Langmuir physics and demonstrate their dynamical manifestation in the reduced Langmuir wave envelope model, we present an example for which the plasma is one wavelength and the forcing is a prescribed

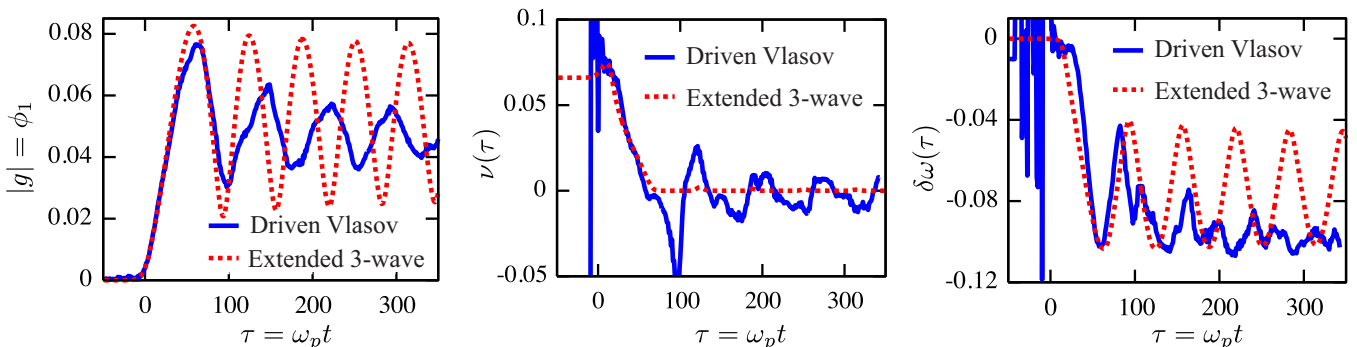


FIG. 3. (Color online) Example of a prescribed ponderomotive drive for $k\lambda_D=0.4$. In the first panel, we see that plasma wave growth is saturated by the nonlinear frequency shift at an amplitude well-predicted by the extended three-wave model. Furthermore, the next two panels show that the dynamic damping and frequency shift are well-predicted by the theory.

function of time. In the reduced description, we solve Eq. (19c) with a chosen right-hand side. We compare results obtained from our extended envelope model to those obtained via a single-wavelength Vlasov simulation; for this case, there is no sideband instability.

In Fig. 3, we present representative results of driven runs using $k_2\lambda_D=0.4$ and $(ck_2/\omega_p)^2 a_0 a_1^* = 0.01$, noting that similar findings were obtained for different drive strengths and temperatures. The frequency and damping were extracted from the Vlasov results using the method of Ref. 28. In the first panel of Fig. 3, we see the evolution of the Langmuir amplitude, as it first grows and then saturates due to the nonlinear frequency detuning from the drive. After the peak, we see subsequent long-time-scale amplitude oscillations due to frequency difference between the Langmuir wave and the drive.

In the second two panels of Fig. 3, we see how the evolving damping and frequency shift give rise to these dynamics. As the particles oscillate and phase-mix in the wave, the damping decreases from the level given by Landau while the frequency of the wave decreases. Furthermore, we see that the simple model for this effect described above closely mimics the dynamics observed in the Vlasov simulation.

B. Application to plasmas relevant to inertial confinement fusion

In the preceding section, we saw that the essential Langmuir wave dynamics was captured by our reduced envelope description including a nonlinear, dynamic damping and frequency shift. Here, we couple this plasma model to the lasers and compare the resulting extended three-wave model of Raman backscatter to a code solving the full Vlasov–Maxwell system. For definiteness, we take parameters relevant to single speckle experiments from the Trident laser (see, e.g., Ref. 29). These experiments observed an increase in the backscatter from that predicted by linear theory using a fixed level of Landau damping. Their interpretation, supported by subsequent kinetic simulations,^{5,7,30} was that the nonlinear phase-mixing of the distribution function resulted in the decrease in Landau damping as we have discussed, leading to an enhanced level of reflected light.

We show the results of both the Vlasov and reduced model in Fig. 4, with the plasma chosen to be $75\ \mu\text{m}$ long, with a density $n_0=10^{20}\ \text{cm}^{-3}$ and temperature $T_e=0.5\ \text{KeV}$, so that $k\lambda_D\approx 0.35$. In the top panel, we see an increase in total reflected light over 10 ps to levels far exceeding the linear, steady-state model. This is the so-called kinetic inflation/enhancement observed by previous authors, which is well-predicted by our model. In the second panel, we show the time history for the case in which $I=2\times 10^{15}\ \text{W/cm}^2$. In this case, the time history of the Vlasov plasma is well modeled by the reduced description up to about 4 ps. After this point, the Vlasov code has one more burst of reflected light while the reduced description has at least two. We believe that this occurs as the trapped particle instability becomes operative, as was proposed in Ref. 6, since for later times we observe the shearing of phase-space holes and the growth of frequency content at $\omega_p \pm \omega_B$ that is characteristic of the trapped particle instability.

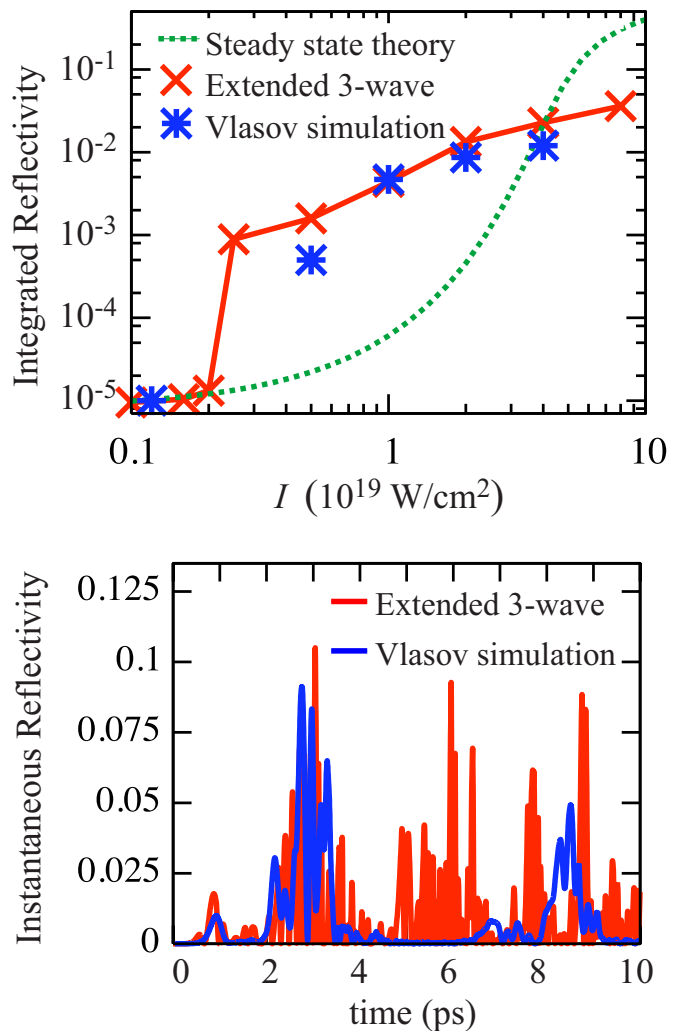


FIG. 4. (Color online) Reflectivity of 527 nm incident light for a $75\ \mu\text{m}$, $n_0=10^{20}/\text{cm}^3$, 0.5 KeV plasma ($k\lambda_D\approx 0.35$). The top panel shows reflectivity integrated over 10 ps, which for intensities between 3×10^{15} and $2\times 10^{15}\ \text{W/cm}^2$ is significantly higher than that predicted by linear theory with constant Landau damping. Note that the reduced model well predicts the scalings observed in the Vlasov code. The second panel shows the time history for $I=2\times 10^{15}\ \text{W/cm}^2$, for which the reflected light comes in bursts with no steady state. The burst seen in the reduced model near 5 ps is apparently suppressed in the Vlasov case by the trapped particle instability.

V. CONCLUSIONS

We have presented a reduced envelope model of slowly driven Langmuir waves including some kinetic effects by exploiting two limiting states of the distribution function: The initial state (described by a frequency and damping derived via the Landau dispersion relation) and the time asymptotic, phase-mixed state (for which the damping vanishes while the frequency becomes a nonlinear function of the amplitude). Associated with the asymptotic distribution function is an incoherent energy of phase-mixing; we take the ratio of the dynamically damped energy to this asymptotic, phase-mixed energy to represent the degree of phase-mixing, and then we use this ratio and simple interpolation to determine the dynamic, nonlinear frequency and

damping of the Langmuir wave. Finally, we compare predictions of our simplified model to Vlasov simulations, finding that it indeed captures much of the relevant physics.

ACKNOWLEDGMENTS

This work was supported by the Lawrence Livermore University Education Partnership Program, by Department of Energy Grant No. DE-FG02-04ER41289, and by the NNSA under the SSAA Program through DOE Research Grant No. DE-FG5207NA28122.

- ¹T. M. O'Neil, *Phys. Fluids* **8**, 2255 (1965).
²I. B. Bernstein, J. M. Greene, and M. D. Kruskal, *Phys. Rev.* **108**, 546 (1957).
³D. S. Montgomery, J. A. Cobble, J. C. Fernandez, R. J. Focia, R. P. Johnson, N. Renard-LeGalloudec, H. A. Rose, and D. A. Russell, *Phys. Plasmas* **9**, 2311 (2002).
⁴D. H. Froula, L. Divol, A. A. Offenberger, N. Meezan, T. Ao, G. Gregori, C. Niemann, D. Price, C. A. Smith, and S. H. Glenzer, *Phys. Rev. Lett.* **93**, 035001 (2004).
⁵H. X. Vu, D. F. DuBois, and B. Bezzerides, *Phys. Plasmas* **9**, 1745 (2002).
⁶S. Brunner and E. J. Valeo, *Phys. Rev. Lett.* **93**, 145003 (2004).
⁷L. Yin, W. Daughton, B. J. Albright, K. J. Bowers, D. S. Montgomery, and J. L. Kline, *Phys. Plasmas* **13**, 072701 (2006).
⁸V. M. Malkin, G. Shvets, and N. J. Fisch, *Phys. Rev. Lett.* **22**, 4448 (1999).
⁹N. J. Fisch and V. M. Malkin, *Phys. Plasmas* **10**, 2056 (2003).
¹⁰D. S. Clark and N. J. Fisch, *Phys. Plasmas* **10**, 4848 (2003); M. S. Hur, R. R. Lindberg, A. E. Charman, J. S. Wurtele, and H. Suk, *Phys. Rev. Lett.* **95**, 115003 (2005).
¹¹W. Cheng, Y. Avitzour, Y. Ping, S. Suckewer, N. J. Fisch, M. S. Hur, and J. S. Wurtele, *Phys. Rev. Lett.* **94**, 045003 (2005).
¹²E. A. Williams, B. I. Cohen, L. Divol, M. R. Dorr, J. A. Hittinger, D. E. Hinkel, A. B. Langdon, D. H. Froula, and S. H. Glenzer, *Phys. Plasmas* **11**, 231 (2004).
¹³H. X. Vu, D. F. DuBois, and B. Bezzerides, *Phys. Plasmas* **14**, 012702 (2007).
¹⁴B. I. Cohen, E. A. Williams, and H. X. Vu, *Phys. Plasmas* **14**, 102707 (2007).
¹⁵D. Bénisti and L. Gremillet, *Phys. Plasmas* **14**, 042304 (2007).
¹⁶G. J. Morales and T. M. O'Neil, *Phys. Rev. Lett.* **28**, 417 (1972).
¹⁷R. L. Dewar, *Phys. Fluids* **15**, 712 (1972).
¹⁸R. R. Lindberg, A. E. Charman, and J. S. Wurtele, *Phys. Plasmas* **14**, 122103 (2007).
¹⁹P. L. Similon and J. S. Wurtele, *Phys. Lett. A* **153**, 224 (1991).
²⁰K. Nishikawa and M. Wakatani, *Plasma Physics* (Springer-Verlag, New York, 2000).
²¹H. A. Rose and D. A. Russell, *Phys. Plasmas* **8**, 4784 (2001).
²²R. R. Lindberg, Ph.D. thesis, University of California (2007).
²³J. R. Cary, D. F. Escande, and J. L. Tennyson, *Phys. Rev. A* **34**, 4256 (1986).
²⁴A. I. Neishtadt, *Sov. J. Plasma Phys.* **12**, 568 (1986).
²⁵R. L. Dewar, *Phys. Fluids* **16**, 431 (1973).
²⁶D. R. Nicholson, *Introduction to Plasma Theory* (Wiley, New York, 1983).
²⁷V. E. Zakharov and V. I. Karpman, *Sov. Phys. JETP* **16**, 351 (1963).
²⁸B. I. Cohen and A. N. Kaufman, *Phys. Fluids* **20**, 1113 (1972).
²⁹J. L. Kline, D. S. Montgomery, B. Bezzerides, J. A. Cobble, D. F. DuBois, R. P. Johnson, H. A. Rose, L. Yin, and H. X. Vu, *Phys. Rev. Lett.* **94**, 175003 (2005).
³⁰D. J. Strozzi, E. A. Williams, A. B. Langdon, and A. Bers, *Phys. Plasmas* **14**, 013104 (2007).